



## $\beta$ -Lactoglobulin as a potential carrier for bioactive molecules

S. Świątek<sup>a</sup>, P. Komorek<sup>a</sup>, G. Turner<sup>b</sup>, B. Jachimska<sup>a,\*</sup>

<sup>a</sup> Polish Academy of Sciences, Jerzy Haber Institute of Catalysis and Surface Chemistry, Niezapominajek 8, Cracow 30-239, Poland

<sup>b</sup> Department of Chemical and Process Engineering, University of Strathclyde, James Weir Building, 75 Montrose Street, Glasgow, UK

### ARTICLE INFO

#### Article history:

Received 27 September 2018

Received in revised form 17 December 2018

Accepted 18 December 2018

Available online 20 December 2018

#### Keywords:

$\beta$ -Lactoglobulin adsorption

Tetracaine

$\beta$ -Lactoglobulin complex

Zeta potential

QCM-D

### ABSTRACT

In this study, the interaction and binding behavior of anesthetic tetracaine (TET) with bovine  $\beta$ -lactoglobulin (LGB) isoform A and a mixture of isoforms A and B were investigated under varying environmental conditions (pH, ionic strength, concentration, LGB-TET complex molar ratio). A wide range of analytical techniques (dynamic light scattering (DLS), electrophoretic mobility, UV-Vis spectroscopy, circular dichroism (CD), quartz crystal microbalance (QCM-D)) were used to analyze the physicochemical properties of the complexes in bulk solution and on the surface of gold. The experiments revealed that TET, which is amphiphilic, could bind with LGB not only in the  $\beta$ -barrel but also onto the surface. The zeta potential of the LGB becomes more positively charged upon interaction with TET due to electrostatic interaction of the amino group present in the TET structure. Changes in the zeta potential values are mostly visible above pH 6 for all tested systems. CD spectra show that interaction with the ligand does not change the secondary structure of the protein. The physicochemical properties of LGB-TET complex were examined in an adsorbed state on a gold surface using the QCM-D method. Additionally, molecular docking was used to evaluate the most likely binding site for TET with LGB.

© 2018 Published by Elsevier B.V.

### 1. Introduction

Bovine  $\beta$ -lactoglobulin (LGB) is one of the most interesting transport proteins with significant importance in the pharmaceutical and food industries. This protein is responsible for the uptake and transportation of hydrophobic molecules such as retinol or fatty acids and their derivatives [1–8]. The central structural element of the protein is the  $\beta$ -barrel, a hydrophobic ligand-binding pocket [9]. The ligand binding mechanism inside the  $\beta$ -barrel is pH dependent and referred to as the Tanford transition [10]. The Tanford transition consists of the reversible change of conformation from one of the loops surrounding the entrance to the  $\beta$ -barrel. At pH > 7.1, the loop “opens” the entrance to the binding site, whereas at pH < 7.1 the change in the loop conformation prevents access to the  $\beta$ -barrel [11]. Crystallographic studies of the bovine  $\beta$ -lactoglobulin complex with vitamin D<sub>3</sub> confirmed the presence of a second binding site on the surface of the protein [12]. Also, intrinsic fluorescence quenching studies have shown that this protein can bind several molecules simultaneously [13]. The research so far focuses mainly on the study of effectiveness complexes formation and their properties. The physicochemical properties were examined in the electrolyte solution and adsorbed state on the model surface. The phenomenon of protein adsorption is a typical process that can support or prevent complexes formation [14–19]. The protein during adsorption adopts a specific orientation what causes that it can expose or block

the binding site. Previous studies of LGB adsorption on the surface of gold allowed the selection of optimal conditions for the study of bovine  $\beta$ -lactoglobulin complexes with bioactive molecules [20,21]. Tetracaine (TET) was selected for the study because it belongs to anesthetics used in ophthalmology and dentistry [22,23]. This drug forms complexes with bovine  $\beta$ -lactoglobulin, in which one binding site inside the  $\beta$ -barrel was located using crystallographic methods [24]. Molecular modeling and crystallographic studies indicate  $\beta$ -lactoglobulin has binding sites inside the  $\beta$ -barrel and on the surface of the protein [13,25–27].

In this study, several complementary experimental methods were used to form a complete understanding of the protein-ligand complex formation; these include: UV-vis spectroscopy, laser Doppler velocimetry (LDV), circular dichroism (CD), quartz microbalance with energy dissipation monitoring (QCM-D). In recent years, computation methods such as density functional theory (DFT) or molecular dynamics (MD) have become increasingly popular for deriving, representing and manipulating the structure and behavior of molecules [24,28–32]. Molecular modeling allows mimicking the structure and behavior of molecules [33–35]. In the case of drug delivery, a computational method used to predict and visualise the predominate binding mode of a ligand with a protein with known three-dimensional structures is molecular docking [36,37]. DFT method is useful for the optimizing the ed structure of molecules and/or estimating the interaction between molecules and surfaces [38–41]. Molecular modeling and crystallographic studies indicate  $\beta$ -lactoglobulin has binding sites inside the  $\beta$ -barrel and on the surface of the protein [13,25–27].

\* Corresponding author.

E-mail address: [ncjachim@cyf-kr.edu.pl](mailto:ncjachim@cyf-kr.edu.pl) (B. Jachimska).

From molecular docking, the interactions between TET and LGB have been simulated providing a visualisation of the complex at an atomic level, the potential binding site of TET with LGB and predicted free energies for each predicted conformation. The molecular docking also helps verify the results produced by the analytical methods used above.

## 2. Materials and methods

### 2.1. Materials

Tetracaine (amethocaine) is a benzoate ester with a molecular weight equal to 264.396 g/mol. It has two amino groups and therefore, it can exist as a monocation or a dication depending on the acidity of environmental conditions. Its acid dissociation constants are  $pK_1 = 2.24$  and  $pK_2 = 8.39$ , respectively [42]. Tetracaine is a powerful anesthetic because it causes loss of sensation by preventing the nerve impulses from being transmitted.

Bovine  $\beta$ -lactoglobulin isoform A (LGB-A) (purity  $\geq 90\%$ ), a mixture of bovine  $\beta$ -lactoglobulin isoforms A and B (LGB-AB) (purity  $\geq 90\%$ ) and tetracaine hydrochloride (TET) used in the study were purchased from Sigma-Aldrich. The protein and ligand solutions were prepared in sodium chloride (NaCl) or phosphate buffer (PB).

The adsorption of LGB and the LGB-TET complexes was performed using a quartz sensor covered by a gold layer. Before every measurement, the sensor was cleaned in piranha solution for 5 min ( $H_2SO_4:H_2O_2:H_2O = 1:1:1$ ), then the sensor was washed by water, and after that, it was heated at  $75^\circ C$  for 30 min. All experiments were carried out at  $25^\circ C$ . The concentration, pH and ionic strength of all solutions were controlled. All other chemicals used were procured from Sigma-Aldrich.

### 2.2. UV-vis measurements

UV-vis measurements were carried out using an Evolution 200 (Thermo Scientific) spectrometer. Measurements were performed for different concentrations of protein and complexes in NaCl or phosphate buffer solution at an ionic strength of  $I = 0.01$  M at  $pH = 7.5$ . Quartz cuvettes with an optical path length of 1 cm were used for all experiments. Absorption spectra were recorded in the wavelength range 190–500 nm, at a 2 nm aperture, with a 1 nm data collection gap, the integration time was 0.1 s, and the scanning speed was 600 nm/min.

### 2.3. Electrophoretic mobility measurements

The electrophoretic mobility of LGB-A, LGB-AB molecules and LGB-A-TET and LGB-AB-TET complexes in NaCl solutions were determined using Zetasizer Nano ZS (Malvern) apparatus. The concentrations of proteins and complexes solutions were 1000 ppm at a controlled ionic strength of  $I = 0.01$  M in the pH range 2–10. Electrophoretic measurements were performed for a molar ratio of protein to the ligand of 1:1 for both complexes. LGB-A-TET electrophoretic measurements were also performed for the molar ratios: 1:2, 1:10, 1:25 and 1:50 of LGB-A to TET, respectively. Applied voltages cause charged particles to migrate to the oppositely charged electrodes. Electrophoretic mobility ( $\mu_e$ ) can be expressed by particles' velocity. The zeta potential of samples was calculated, using Henry's eq. (1):

$$\xi = \frac{3\eta\mu_e}{2\epsilon f(\kappa a)} \quad (1)$$

where  $\xi$  is zeta potential,  $\epsilon$  is the dielectric constant of water,  $\eta$  is the solution viscosity,  $f(\kappa a)$  is the function of the dimensionless parameter  $\kappa a$ .

### 2.4. Quartz crystal microbalance with energy dissipation monitoring (QCM-D)

The formation process of complexes and the effectivity of their adsorption was monitored using quartz microbalance with the monitored dissipation of energy (QSense E1) with a flow module. A constant flow speed of  $500 \mu l \text{ min}^{-1}$  was used throughout the experiment. The flow was controlled by a peristaltic pump (Ismatec). Sensors with gold electrode surfaces were used for all experiments. The baseline was determined by the flow of the NaCl solution at the specified ionic strength and pH for 10 min. In the QCM-D method, the adsorbed mass ( $\Delta\Gamma$ ) for rigid, uniform films is directly proportional to the decrease in the resonant frequency of sensor's vibration ( $\Delta f = f - f_0$ ) according to Sauerbrey model(2):

$$\Delta\Gamma = -C \frac{\Delta f}{n} \quad (2)$$

where  $C$  is the crystal constant for quartz (equal to  $17.7 \text{ ng cm}^{-2}$ ), and  $n$  is the overtone number.

### 2.5. Circular dichroism measurements

Circular Dichroism (CD) measurements were carried out using a Jasco J-1500 spectrometer. Solvent baseline measurements were taken using NaCl  $I = 10^{-2}$  M before the CD spectra of LGB and LGB-TET complex at different pH values were acquired. The concentration of LGB was maintained at 100 ppm. Spectra were recorded over a range of 200–250 nm with a scan speed of 50 nm/min and a bandwidth of 1 nm using a quartz cuvette with a path length of 0.5 cm.

### 2.6. Molecular docking

In this research, the interaction between TET and LGB was simulated to investigate whether TET binds with LGB and subsequently, determine the predominant binding location of TET on LGB. The 3D chemical structures of LGB in a  $pH = 7.5$  (IDs: 3NPO) was retrieved through the RCSB Protein Data Bank. The 3D structure of TET was sourced from the Drug Bank. The chemical structures of protein and ligand were analysed and fully optimized using the molecular structure and beautify tool and docked to each other through Scigress v12.12.0.0 software. The molecular docking software uses a genetic algorithm coupled with a knowledge-based scoring function – PMF04 – to simulate the interactions between TET and LGB anywhere at the protein surface and within cavities and then rank the potential poses based on their predicted free energies (free energies must be negative for the potential conformation to exist). Initial blind docking simulations with the protein side chains assumed rigid and the ligand assumed flexible were carried out, the binding site was shown to be at the entrance/partially within the LGB antiparallel  $\beta$ -barrel. After careful consideration of the simulations produced by blind docking – the whole protein was considered as the active site – and reference to literature, a  $20 \times 20 \times 20$  box around the MET107 amino acid was chosen as an appropriate active site to encompass the entrance and cavity of the antiparallel  $\beta$ -barrel, reducing the search space. The remaining simulations were all ran with a grid spacing of  $0.25 \text{ \AA}$ , flexible ligand and protein, convergence RMSD of  $< 1$ , unite atom on and amber van der Waals off. The other parameters were all set based on the number of conformational searches and thus the speed of the simulation – this was heavily dependent on computational power.

## 3. Results and discussion

### 3.1. Physicochemical characteristics $\beta$ -lactoglobulin in bulk solution

According to literature data, the bovine  $\beta$ -lactoglobulin has a  $\beta$ -barrel within its structure. The barrel is open or closed depending on

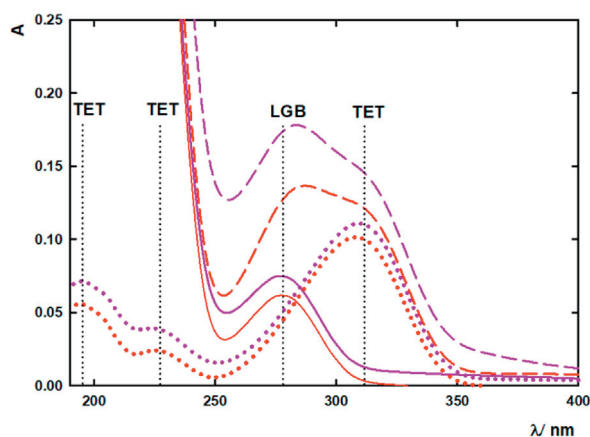
environmental conditions, and the opening and closing process is defined as the Tanford transition [29,30]. The measurements were carried out at pH = 5.5 when the EF loop closes the entrance to the  $\beta$ -barrel, and at pH = 7.5 when there is open access to the binding site of bovine  $\beta$ -lactoglobulin. Firstly, the UV-vis spectra for LGB, TET and LGB-TET complexes in 0.01 M NaCl in pH = 5.5 and 7.5 were recorded (Fig. 1). UV-vis absorption spectroscopy is a straightforward method which is used to check whether there are structural changes for molecules in solution dependent on environmental conditions. The concentration of LGB and TET was 5  $\mu$ M and the molar ratio of LGB:TET was 1:1. The maximum for LGB is observed at 279 nm, which is characteristic for proteins possessing tryptophan and tyrosine. For tetracaine, three peaks centered at wavelength 195, 227 and 310 nm were recorded, which is consistent with work by M.A. Nouairi et al. [43]. The effect of the Tanford transition is particularly visible at 279 nm, but higher absorption at pH = 5.5 and changes in the shape of the spectrum in comparison with measurements at pH = 7.5 are present in the whole featured wavelength range. There is also higher absorption observed for the tetracaine spectrum at pH = 5.5. The result is associated with higher protonation of ligand molecules in lower pH. What is more, strong dissimilarity in the shape of complex spectra indicate the differences in interactions between bovine  $\beta$ -lactoglobulin and tetracaine under various pH conditions.

The structure of the LGB molecule based on the CD spectrum obtained in the 0.01 M NaCl solution and pH range 3.0 to 9.0 is very similar and is presented as follows:  $\beta$ -sheet, 40.4%;  $\beta$ -turns, 13.3%;  $\alpha$ -helices, 13.7%; and random coil, 32.6%. For comparison secondary structures of LGB based on the crystallographic structure (PDB ID: 1BSY) present:  $\beta$ -sheet 40%;  $\beta$ -turns 14%;  $\alpha$ -helices 19%; and random coil 27%. Additionally, CD measurements show no significant structural changes after ligand binding to the LGB structure for both conditions, at pH 5.5 and 7.5 (Fig. 1b).

The efficiency of the LGB complexes formation with tetracaine was monitored using UV-vis spectroscopy. The recorded spectra for LGB-A-TET complexes in a molar ratio of 1:1–1:10 are shown in Fig. 2. UV-vis spectrum maxima were observed in the 278 nm for LGB and 310 nm range for TET. The addition of different concentrations of TET caused an increase in absorption and is associated with a red shift, what indicates the formation of the LGB-A complexes with TET.

The binding constant  $K_{UV-vis}$  was determined from the dependence  $1/\Delta A$  on  $1/C_{TET}$  (Fig. 1b). The dependence is linear; the constant  $K_{UV-vis}$  equals the ratio of the intersection point and the slope of the straight line [30]:

$$K_{UV-vis} = \frac{\text{intercept}}{\text{slope}} \quad (3)$$



a

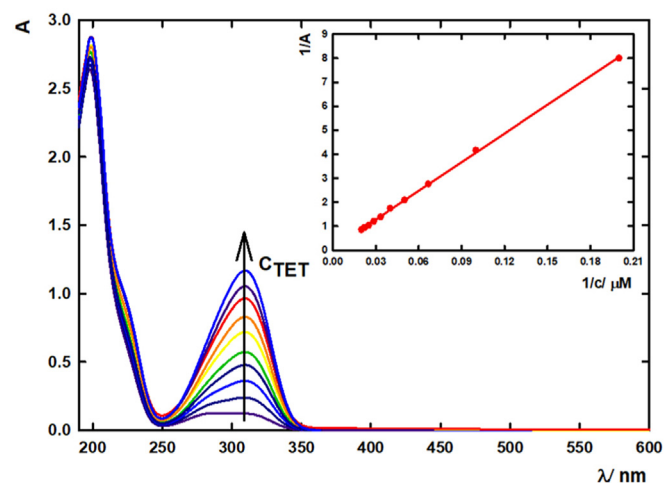
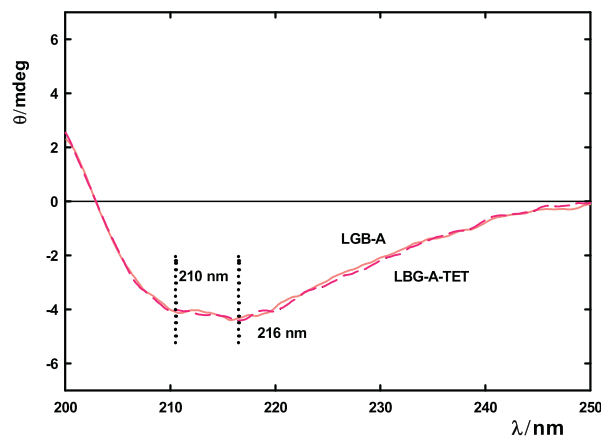


Fig. 2. a) UV-vis spectrum for LGB-TET complexes,  $C_{LGB} = 5 \mu\text{M}$  (100 ppm),  $C_{TET} = 5, 10, 15, 20, 25, 30, 35, 40, 45$  and  $50 \mu\text{M}$  ( $I = 0.01$  M PB, pH = 7.5, 25 °C, b) dependence  $1/A$  on  $1/C_{TET}$ .

The determined value of  $K_{UV-vis}$  is  $0.22 \times 10^4 \text{ M}^{-1}$ , is lower than the constant values for antibiotics determined by Mehraban equal to 2.0 and  $0.7 \times 10^4 \text{ M}^{-1}$  for ciprofloxacin and kanamycin [30]. The binding constant in the case of antibiotics concern binding of the active molecule to the outside of the protein structure. In the case of tetracaine, we are dealing with a molecule which can be incorporated into the hydrophobic internal structure or on the surface of the protein. The lower binding constant for tetracaine is related to the hydrophobic interactions, which are dominant in this case, being lower than the electrostatic interactions which are responsible for the formation of complexes bound on the surface of the protein.

The association rate constants determined from the isothermal calorimetry of titration by J. I. Loch is equal  $8.85 \cdot 10^2$  for tetracaine and  $2.48 \cdot 10^5 \text{ M}^{-1}$  for lauric acid [3,24]. Lauric acid is a natural ligand of bovine  $\beta$ -lactoglobulin, and similarly to tetracaine bound inside a barrel, the size is comparable to TET. Association constants for selected ligands determined by various methods are summarized in Table 1.

In general, association constants are higher when the ligand binds inside the barrel than when they bind on the outside. Association constants in the range  $10^2$ – $10^4 \text{ M}^{-1}$  are very weak interactions compared to the formation of LGB complexes with fatty acids, which are natural ligands and therefore have the highest affinity. The



b

Fig. 1. a) UV-vis spectra of LGB-A (solid), TET (dotted) and LGB-A-TET 1:1 complex (dashed). The results recorded at pH = 5.5 are presented in purple, at pH = 7.5 in red, b) CD spectra of LGB-A and LGB-A-TET at pH 7.5 for  $I = 1 \times 10^{-2}$  M NaCl and  $c = 100$  ppm.

**Table 1**  
Comparison of association constants ( $K_a$ ) of bovine  $\beta$ -lactoglobulin complexes formation determined using various experimental methods.

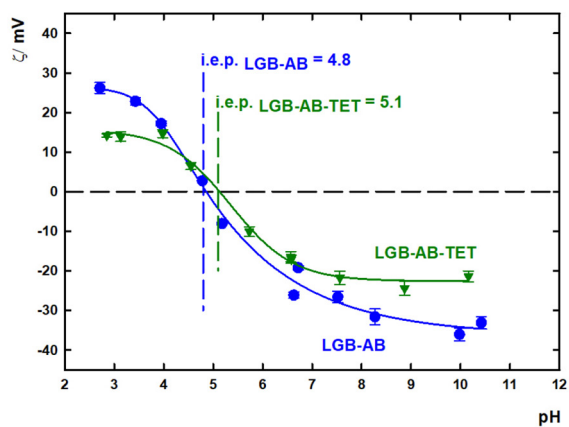
Ligand	Method	$K_a$ [ $M^{-1}$ ]
Tetracaine [24]	ITC	$8.85 \cdot 10^2$
Pramocaine [24]	ITC	$3.00 \cdot 10^3$
Lauric acid [44]	ITC	$2.48 \cdot 10^5$
Oxaliplatin [45]	ITC	$1.55 \cdot 10^3$
Oxali-palladium [45]	ITC	$3.30 \cdot 10^3$
Doxorubicin [46]	ITC	$1.00 \cdot 10^4$
N-(trifluoroacetyl) doxorubicin [46]	ITC	$2.50 \cdot 10^4$
Norfloxacin [6]	ITC	$1.70 \cdot 10^3$
Sodium dodecyl sulfate [47]	ITC	$8.38 \cdot 10^5$
Dodecyltrimethylammonium chloride [47]	ITC	$0.57 \cdot 10^5$
Chlorpromazine [7]	Spectrofluorimetry	$24.0 \cdot 10^3$
Piperine [48]	CD	$8.00 \cdot 10^4$

affinity for binding of positively charged ligands is lower than their neutral counterparts due to the positively charged amino acid groups at the entrance of the LGB beta barrel. In this case, the integration of TET into the barrel is sterically hindered.

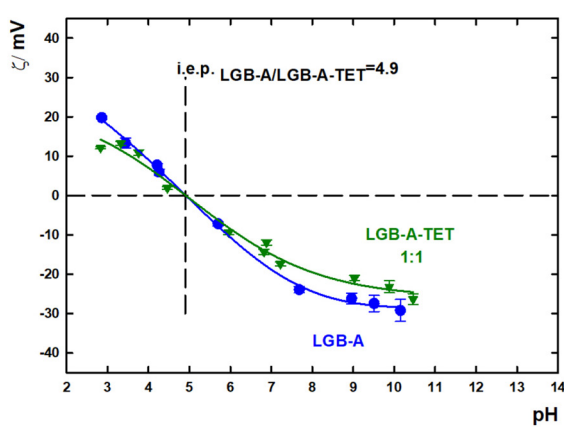
### 3.2. Effective charge of a complex of $\beta$ -lactoglobulin with tetracaine

Tetracaine molecules are amphiphilic and therefore, can be incorporated into both the hydrophobic pocket and the surface of the protein through electrostatic interactions due to the amino group present in the structure. The most useful method to precisely determine changes in in-situ experiments on surface charge for solid/liquid interfaces is electrophoretic mobility. This method can be used for optimization or following the interaction for an extensive range of systems [49–51]. Electrophoretic mobility measurements allowed the determination of the value of the zeta potential of both proteins and the formed complexes. To identify the TET quantification on the surface of the protein, the surface charge of the protein was measured after complex formation with TET. The changes in the zeta potential of protein molecules and complexes formed (molar ratio of protein to ligand equal to 1:1) were calculated using the Henry Formula (1). The Hückel approximation:  $f(\kappa\alpha) = 1$ , was used for the calculations.

The dependences of changes in zeta potential values for the measured systems from the pH solution at 0.01 M NaCl are shown in Fig. 3. The zeta potential for LGB-AB molecules varies from  $-34.2$  to  $26.1$  mV, while for the formed complex in the range from  $-21.4$  to  $14.2$  mV. The zeta potential of the LGB-AB-TET complex molecules is 5 mV lower in value than for LGB-AB at pH 7.5. The isoelectric point determined (i.e.p.) is shifted towards higher pH values and is equal to 5.1. For LGB-A, however, the zeta



a



b

**Fig. 3.** Zeta potential dependence for a) mixture of LGB-AB isoforms and b) isoform A and their complexes with tetracaine. The points on the graph represent experimental data, lines fitting to the experimental data. Zeta potential values for LGB and LGB A + B isoforms are marked in blue, while complexes in green. The dashed lines indicate the isoelectric point.

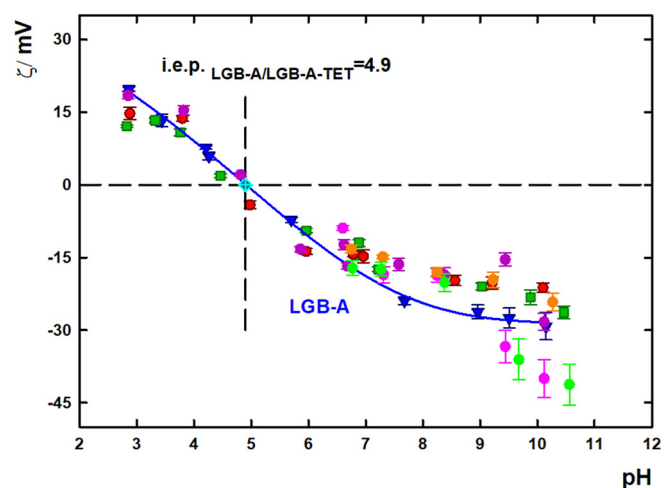


**Fig. 4.** The dependence of the zeta potential for LGB-A (blue) and LGB-A-TET complexes from the solution pH for ionic strength  $I = 0.01$  M. The LGB-A-TET complexes were determined as 1:1 (green), 1:2 (red), 1:10 (purple), 1:15 (orange), 1:25 (light green), 1:50 (pink), the isoelectric point is marked with a dashed line.

potential varies between  $-29.2$  to  $19.8$  mV, and LGB-A-TET  $-26.3$  to  $12.1$  mV. The difference in the zeta potential between LGB-A and LGB-A-TET at  $pH = 7.5$  is twice lower than for the LGB-AB and LGB-AB-TET systems and amounts to 2.5 mV. The isoelectric point for LGB-A and LGB-A-TET remains unchanged and is located at  $pH 4.9$ . The zeta potential value of the complexes is more positive than the zeta potential for a protein, which suggests that tetracaine molecules bind to the surface of the protein. Fig. 4 shows the dependence of the zeta potential on the pH for the complex LGB-A-TET in a different molar ratio.

The values of zeta potential for complexes in a molar ratio of 1:1, 1:2, 1:10 and 1:15 is similar. Changes in the zeta potential value are visible for  $pH$  above 6 for all tested complexes. A significant excess of TET relative to the LGB-A (1:25 and 1:50) results in a significant decrease of the zeta potential at  $pH > 9$  to a value of  $-40 \pm 5$  mV, and it is associated with the tendency of the protein to aggregation.

### 3.3. Self-assembly of $\beta$ -lactoglobulin complexes on gold surface determined by QCM-D

The properties of bovine  $\beta$ -lactoglobulin isoform A and a mixture of isoforms A and B complexes with tetracaine was monitored using



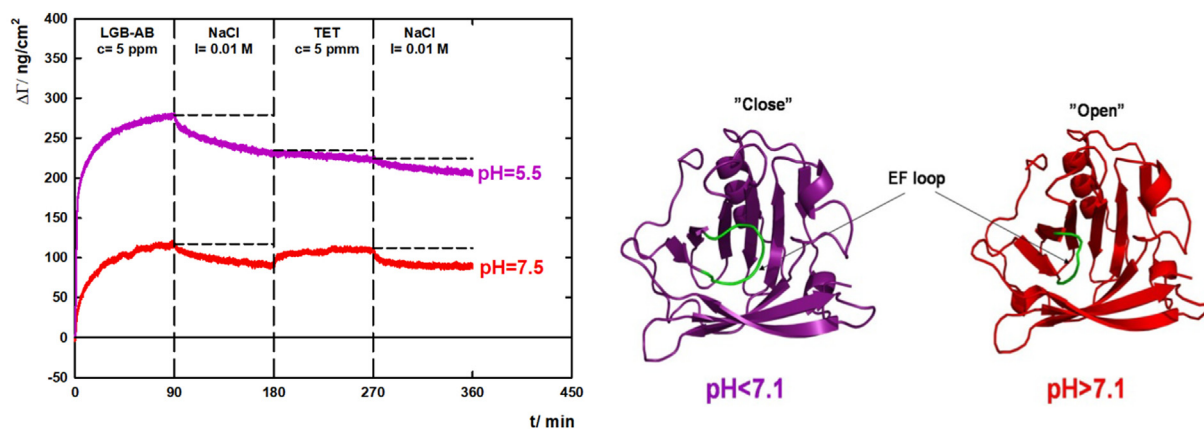


**Fig. 5.** Complexes formation between  $\beta$ -lactoglobulin and tetracaine determined using the QCM-D method. The result for complex LGB-AB-TET formation at pH = 5.5 is shown in violet, while for LGB-AB-TET complex formation at pH = 7.5 is displayed in red. On the graphs, the bovine  $\beta$ -lactoglobulin structure is illustrated, showing the two Tanford transition states; open and closed barrel. The EF loop which opens and closes the  $\beta$ -barrel is marked in green.

Quartz Crystal Microbalance with Dissipation Monitoring. Measurements of complexes formation depending on the pH of the solution were performed at the concentration of protein and ligand equal to 5 ppm in a NaCl solution at ionic strength  $I = 0.01$  M for pH = 5.5 and pH = 7.5. The influence of ionic strength (for  $I = 0.001$  M and  $I = 0.01$  M) on the complex formation was also investigated. The protein adsorption was carried out for 90 min, after that the system was rinsed by NaCl solution at the specified pH and ionic strength for 90 min to observe whether the adsorption of protein to the gold surface was irreversible.

The dependence of mass adsorbed onto the sensor during the formation of LGB-AB-TET complexes under different pH conditions is presented in Fig. 5. There is an increase of mass adsorbed during the introduction of TET solution to the system at pH = 7.5, which indicates the binding of TET to the protein. Due to the low binding constant value ( $K_{UV-vis} = 0.22 \times 10^4 \text{ M}^{-1}$ ), rinsing causes the removal of TET molecules from the binding site of bovine  $\beta$ -lactoglobulin. Whereas, during the addition of TET at pH = 5.5, the increase of adsorbed mass was not observed, which indicates TET molecules do not bind to bovine  $\beta$ -lactoglobulin in such conditions because the entrance to the  $\beta$ -barrel is closed. This is in line with the Tanford transition phenomenon, which is controlled by pH and includes a change of EF loop conformation occurring at the pH = 7.1. The number of LGB-A molecules adsorbed onto the gold surface, and the number of TET molecule bonded to LGB-A was calculated using the following equation:

$$N = \frac{\Gamma^{QCM} \cdot N_A}{M_w} \quad (4)$$

where:  $N$  is a number of molecules,  $\Gamma^{QCM}$  is adsorbed mass,  $M_w$  is molecular mass,  $N_A$  is Avogadro's number.

The number of TET molecules per one molecule of LGB-AB for an ionic strength of  $I = 0.01$  M is 13 (molecules TET) (Table 2). There is

**Table 2**

The values of adsorbed mass ( $\Gamma$ ) and the number of adsorbed molecules ( $N$ ) of bovine  $\beta$ -lactoglobulin (a mixture of isoforms A and B) and complexes of bovine  $\beta$ -lactoglobulin-TET (LGB-AB-TET) at  $I = 0.01$  M NaCl and pH = 7.5 based on QCM results in calculations.

$\Gamma_{LGB-AB}^{QCM} \text{ ng/cm}^2$	89.8
$\Gamma_{TET}^{QCM} \text{ ng/cm}^2$	19.5
$N_{LGB-AB} \text{ cm}^{-2}$	$2.94 \times 10^{12}$
$N_{TET} \text{ cm}^{-2}$	$3.90 \times 10^{13}$
$N_{LGB-AB}/N_{TET}$	13

only one binding site in the barrel, indicating that the ligand binds not only inside the bovine  $\beta$ -lactoglobulin structure but also to the surface of the protein. According to the zeta potential analysis, the formed complex has a higher zeta potential by 20% in comparison to the zeta potential of  $\beta$ -lactoglobulin. This suggests that some of the TET molecules bind to the surface of the protein, while other TET molecules are located inside the  $\beta$ -barrel of  $\beta$ -lactoglobulin.

The adsorption efficiency of the LGB-AB-TET and LGB-A-TET complexes was measured for complexes formed in a protein to ligand molar ratio of 1: 1 ( $c = 5$  ppm) at pH = 7.5 (when the barrel is open). The ionic strength of the solutions was 0.01 M. Adsorption of the complex was carried out for 90 min, and then the system was rinsed by NaCl solution for the next 90 min. The dependence of adsorbed mass of bovine  $\beta$ -lactoglobulin isoform A and a mixture of bovine  $\beta$ -lactoglobulin isoform A and B and their complexes with tetracaine has been presented in Fig. 6. For the complex formed from the mixture of isoforms, the adsorbed mass is  $74.8 \text{ ng cm}^{-2}$ , while for protein itself the mass is  $89.8 \text{ ng cm}^{-2}$ , which is about 15% difference in adsorbed mass. In this case, results show the lower efficiency of adsorption for the complex in relation to the protein itself. On the other hand, in the case of the bovine  $\beta$ -lactoglobulin isoform A, the value of adsorbed mass is almost identical for the formed protein-ligand complex of LGB-A-TET and protein LGB-A, respectively  $157.1$  and  $150.5 \text{ ng cm}^{-2}$ . The difference in the adsorption efficiency of the formed protein-ligand complexes in relation to the protein itself correlates with their zeta potential values. In the case of the LGB-TET complexes in comparison to the protein itself, the difference in zeta potential is twice lower for LGB-A isoform than for mixture of A and B isoforms. This results in a difference in the effectiveness of the adsorption of the studied complexes for different isoforms of LGB in protein-ligand complexes. The degree of desorption is 23% and 14% for LGB-AB and LGB-A, respectively. In the case of complexes, the desorption is lower, and its value is 7% for LGB-AB-TET and 3% for LGB-A-TET system. The values of desorption indicate that the higher irreversibility of adsorption occurs for LGB-TET complexes compared to the protein itself.

### 3.4. Interaction of tetracaine with $\beta$ -lactoglobulin by molecular docking

In this part of the report, the simulated data obtained shall be analysed to determine whether TET and LGB can form a stable complex, the potential binding location, the important interactions involved in the formation of a complex between TET and LGB and the accuracy of the simulated results. The simulations that will be analysed are the interaction of protonated and unprotonated TET with LGB (PDB ID 3NPO). The simulation of complex formation for both protonated and

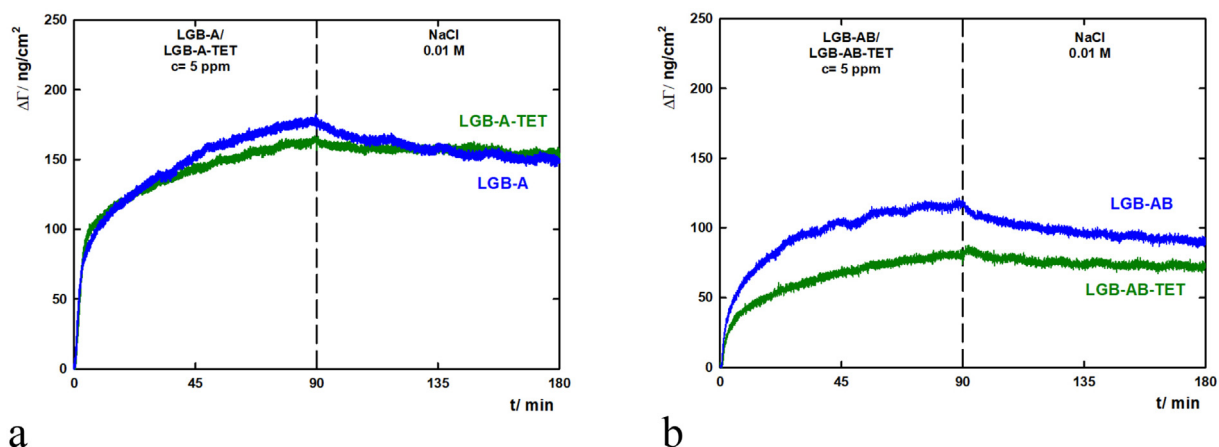


**Fig. 6.** The comparison of the adsorbed mass ( $\Delta\Gamma$ ) of proteins and their complexes with tetracaine as a function of time. The results for proteins are presented in blue, while for protein-ligand complexes are displayed in green a) LGB isoform A and its complex, b) mixture of isoforms A and B and their complexes formed at pH = 7.5 and ionic strength conditions  $I = 0.01$  M.

non-protonated TET produced negative free energies of binding of  $-220.92$  kJ/mol and  $-180.63$  kJ/mol, respectively (Fig. 7).

Therefore, SCIGRESS has predicted complex formation between TET and LGB would proceed, however, the free energies of binding have been grossly overestimated when compared to the isothermal titration calorimetry value of  $-16.7 \pm 0.3$  kJ/mol. Furthermore, SCIGRESS has predicted the predominant binding mode of TET with LGB is within the hydrophobic  $\beta$ -barrel cavity. Agreeing with the previous report by Loch et al. [24]. Additionally, the docking results have further solidified that the primary binding site for LGB is within the hydrophobic  $\beta$ -barrel cavity, which has been intensely investigated and shown for other

ligands. The end amine functional group is orientated towards the entrance of the cavity (i.e., lies within the surrounding solvent) because of the polar nature of the amine and carbonyl functional groups interacting with the surrounding polar solvent. The other amine functional group, benzene ring, and straight chain alkane penetrate within the hydrophobic cavity due to their non-polar nature. The orientation of the TET within the hydrophobic cavity was as expected and agrees with X-ray crystallography by Loch et al. [24]. The amino acid side chains interacting with the protonated TET in the hydrophobic cavity are ILE12, ILE56, ILE71, ILE84, LEU30, LEU46, LEU54, LEU58, LEU103, ASN90, VAL41, VAL43, VAL92, VAL94, MET107, PHE105, and PRO30

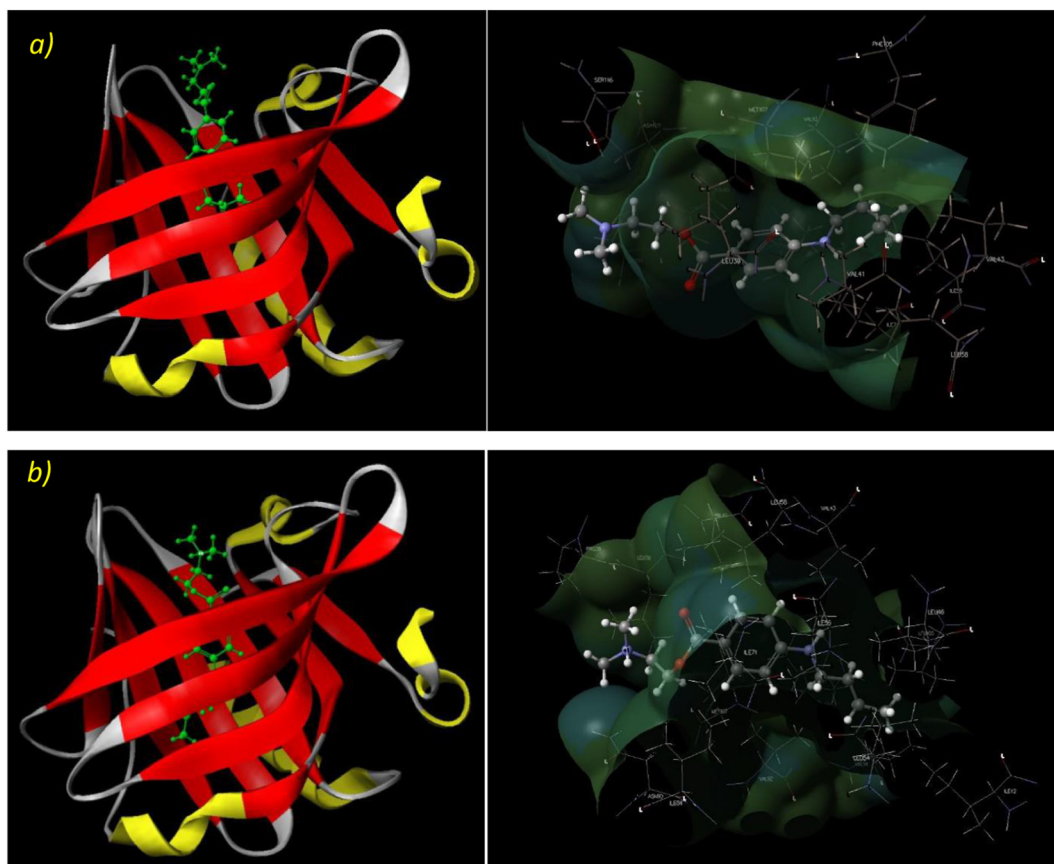


**Fig. 7.** Docked: a) protonated, b) unprotonated TET (Drugbank: DB09085) with LGB (PDB: 3NPO).

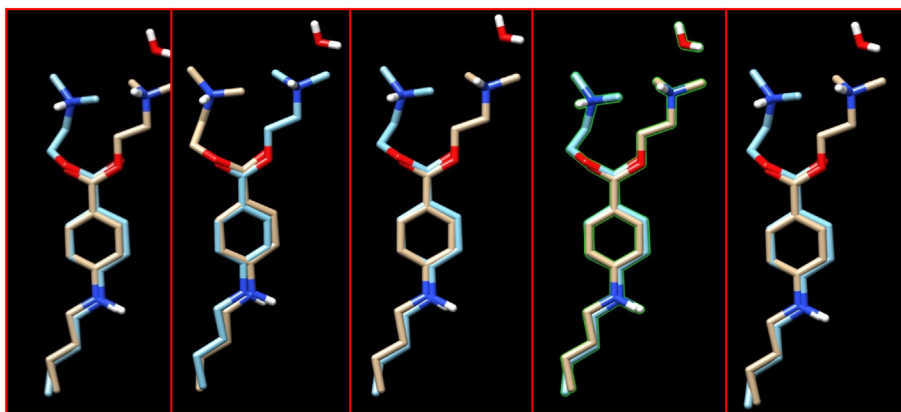


**Fig. 8.** The top 5 scored conformations of protonated TET/LGB complex, from left to right, superimposed on crystal structure (PDB: 4Y0P). The water molecule is part of the crystal structure.

(Fig. 10). The amino acid side chains interacting with the non-protonated TET within the hydrophobic cavity are SER116, ASN88, ASN90, ASN109, ILE56, ILE84, ILE88, VAL92, MET107, PHE105, LEU39, and LEU58. The surrounding amino acid groups for both protonated and non-protonated TET have some similarities. However, the protonated TET penetrated further into the hydrophobic pocket interacting with more amino acid side chains. The predicted complex formation suggests the interactions involved for both protonated and non-protonated TET and the surrounding amino acid groups are entirely van der Waals forces with no hydrogen bonding taking place. The lack of hydrogen bonding appears to disagree with previous research by Loch et al. which will be discussed in the following section [24].

To verify the accuracy of the docking predictions, the top 5 scored conformations for both protonated and non-protonated TET complexed with LGB were superimposed using the software Chimera onto a 3D crystal structure of the complex solved by X-ray crystallography, and the RMSD for the TET molecules were calculated.

The RMSD for the top 5 scored conformations in Fig. 8 were 4.989, 4.961, 4.981 and 4.972, respectively. The best model for protonated TET was the second-ranked conformation. Therefore, the higher scored conformations are not necessarily better. Visually inspecting the superimposed models on the crystal structures in Fig. 8, docking has predicted the non-polar end of the TET accurately. However, the polar end significantly deviates from the natural conformation with the carbon bond attached to the benzene ring rotating 180 degrees on its axis. The most plausible explanation for this deviation was the water molecules were not considered to play an essential role in the binding of TET to LGB. On the contrary, water molecules appear to play a vital role in the formation of a TET/LGB complex in its natural conformation, as the TET and water form a hydrogen bond, as shown by Loch et al. [24].

Furthermore, the report also shows the water molecule forms a hydrogen bond with the amino acid side chain LYS62 and TET form a hydrogen bond with the amino acid side chain PRO38, both of which potentially play an essential role in the formation of a TET/LGB complex in its natural formation. The study by Loch et al. suggests the most critical factor is, in fact, the hydration of the ligands during complex formation with LGB and not ordered molecules within the hydrophobic cavity [24].

The RMSD for the top 5 scored conformations in Fig. 9 were 7.505, 7.489, 7.756, 7.488 and 7.489. The best model for non-protonated TET was the fourth-ranked conformation. Visually inspecting the superimposed models onto the crystal structure in Fig. 9; docking completely deviates from the natural conformation of TET complexed to LGB. Similarly, to the previous section, this can largely be explained by the lack of water involved in the simulation of the complex formation of TET with LGB. Although, the deviation is significantly worse when the nitrogen is no longer protonated.

After comparing the simulated complex formation of TET with LGB and the experimental complex formation of TET with LGB, the grossly overestimated free energies of binding predicted during docking can be explained by the lack of hydration of TET. During the complex formation of TET within the hydrophobic cavity of LGB, the water molecules surrounding the TET will impede the binding to BLG.

#### 4. Conclusion

The UV-vis, QCM-D, in situ electrophoretic mobility measurements and molecular docking simulations, have characterised the mechanisms involved in the interaction between LGB and tetracaine hydrochloride. Immobilization of tetracaine on the surface of the LGB molecule induces

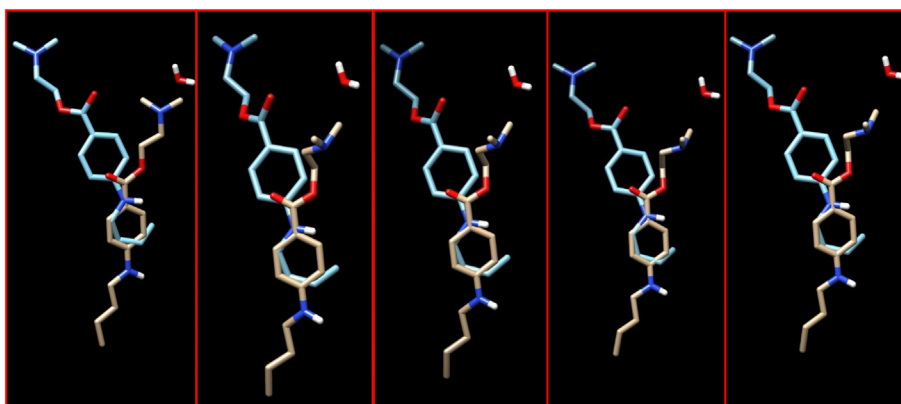


**Fig. 9.** The top 5 scored conformations of non-protonated TET/LGB complex, from left to right, superimposed on crystal structure (PDB: 4Y0P). The water molecule is part of the crystal structure.



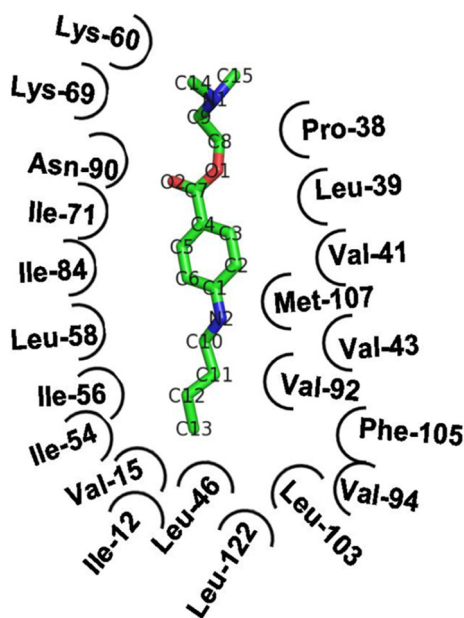


**Fig. 10.** The surrounding amino acid residues are: Lys-60, Lys-69, Val-15, Val-41, Val-43, Val-92, Val-94, Leu-39, Leu-46, Leu-58, Leu-103, Leu-122, Ile-12, Ile-54, Ile-56, Ile-71, Ile-84, Pro-38, Asn-90, Met-107 and Phe-105.

changes in surface charge of the protein and can be acquired via electrophoretic mobility measurements. Changes in the zeta potential values are mostly visible for  $\text{pH} > 6$ . The zeta potential measurement gives proof that bovine  $\beta$ -lactoglobulin binds tetracaine onto the LGB surface. The change of zeta potential is two times higher for a complex of LGB-AB-TET than for LGB-A-TET. The most effective formation can be obtained for molar ratio 1:10, a higher amount of tetracaine molecules does not cause more bonds. A quantitative interpretation of the formation of LGB-TET complexes was achieved using the QCM-D method. From QCM-D measurement the molar ration LGB to TET is equal to 1:13 and is very close to the result obtained from zeta potential measurement.

Presented results have important practical implications because they demonstrate that that bovine  $\beta$ -lactoglobulin binds ligands both into the  $\beta$ -barrel and onto its surface. The molecular docking of TET with  $\beta$ -LG has suggested binding between the protein and ligand is possible with the most likely binding site with the hydrophobic cavity, confirming the results produced by the analytical methods in this study and agreeing with literature. However, the prediction of the free binding energies are greatly overestimated, and the orientation of the TET within the cavity was inaccurate most likely due to not considering the hydration of TET in the simulations, an essential factor in binding between TET and LGB shown in the literature.

## Acknowledgment

The presented work was partially supported by Grant NCN OPUS2016/23/B/ST5/0278. This work was partially supported by Grant POWR03.02.0000-1013/16.

## References

- G. Kontopidis, C. Holt, L. Sawyer, Invited review:  $\beta$ -lactoglobulin: binding properties, structure, and Function, *J. Dairy Sci.* 87 (2004) 785–796, [https://doi.org/10.3168/jds.S0022-0302\(04\)73222-1](https://doi.org/10.3168/jds.S0022-0302(04)73222-1).
- L. Sawyer, G. Kontopidis, The core lipocalin, bovine  $\beta$ -lactoglobulin, *Biochim. Biophys. Acta - Protein Struct. Mol. Enzymol.* 1482 (2000) 136–148, [https://doi.org/10.1016/S0167-4838\(00\)00160-6](https://doi.org/10.1016/S0167-4838(00)00160-6).
- J. Loch, A. Polit, A. Górecki, P. Bonarek, K. Kurpiewska, M. Dziedzicka-Wasylewska, K. Lewiński, Two modes of fatty acid binding to bovine  $\beta$ -lactoglobulin—crystallographic and spectroscopic studies, *J. Mol. Recognit.* 24 (2011) 341–349, <https://doi.org/10.1002/jmr.1084>.
- K. Sakurai, Y. Goto, Manipulating monomer-dimer equilibrium of bovine  $\beta$ -lactoglobulin by amino acid substitution, *J. Biol. Chem.* 277 (2002) 25735–25740, <https://doi.org/10.1074/jbc.M203659200>.
- K. Sakai, K. Sakurai, M. Sakai, M. Hoshino, Y. Goto, Conformation and stability of thiol-modified bovine  $\beta$ -lactoglobulin, *Protein Sci.* 9 (2000) 1719–1729, <http://www.pubmedcentral.nih.gov/articlerender.fcgi?artid=2144692&tool=pmcentrez&rendertype=abstract>.
- B.K. Paul, N. Ghosh, S. Mukherjee, Binding interaction of a prospective chemotherapeutic antibacterial drug with  $\beta$ -lactoglobulin: results and challenges, *Langmuir* 30 (2014) 5921–5929, <https://doi.org/10.1021/la501252x>.
- J. Bhattacharyya, K.P. Das, Interactions of chlorpromazine with milk proteins, *Mol. Cell. Biochem.* 221 (2001) 11–15, <https://doi.org/10.1023/A:1010847621496>.
- E. Dufour, P. Roger, T. Haertlé, Binding of benzo( $\alpha$ )pyrene, ellipticine, and cis-parinaric acid to  $\beta$ -lactoglobulin: influence of protein modifications, *J. Protein Chem.* 11 (1992) 645–652, <https://doi.org/10.1007/BF01024965>.
- G. Kontopidis, C. Holt, L. Sawyer, The ligand-binding site of bovine  $\beta$ -lactoglobulin: evidence for a function? *J. Mol. Biol.* 318 (2002) 1043–1055, [https://doi.org/10.1016/S0022-2836\(02\)00017-7](https://doi.org/10.1016/S0022-2836(02)00017-7).
- C. Tanford, L.G. Bunville, Y. Nozaki, The reversible transformation of  $\beta$ -lactoglobulin at pH 7.5, *J. Am. Chem. Soc.* 81 (1959) 4032–4036, <https://doi.org/10.1021/ja01524a054>.
- B.Y. Qin, M.C. Bewley, L.K. Creamer, H.M. Baker, E.N. Baker, G.B. Jameson, Structural basis of the tanford transition of bovine  $\beta$ -lactoglobulin *Biochemistry* 37 (1998) 14014–14023, <https://doi.org/10.1021/bi981016t>.
- M.C. Yang, H.H. Guan, M.Y. Liu, Y.H. Lin, J.M. Yang, W.L. Chen, C.J. Chen, S.J.T. Mao, Crystal structure of a secondary vitamin D3 binding site of milk  $\beta$ -lactoglobulin, *Proteins Struct. Funct. Genet.* 71 (2008) 1197–1210, <https://doi.org/10.1002/prot.21811>.
- J. Zhang, X. Liu, M. Subirade, P. Zhou, L. Liang, A study of multi-ligand  $\beta$ -lactoglobulin complex formation, *Food Chem.* 165 (2014) 256–261, <https://doi.org/10.1016/j.foodchem.2014.05.109>.
- K. Nakanishi, T. Sakiyama, K. Imamura, On the adsorption of proteins on solid surfaces, a common but very complicated phenomenon, *J. Biosci. Bioeng.* 91 (2001) 233–244, [https://doi.org/10.1016/S1389-1723\(01\)80127-4](https://doi.org/10.1016/S1389-1723(01)80127-4).
- M. Rabe, D. Verdes, S. Seeger, Understanding protein adsorption phenomena at solid surfaces, *Adv. Colloid Interf. Sci.* (2011), <https://doi.org/10.1016/j.cis.2010.12.007>.
- M. Rabe, D. Verdes, M. Rankl, G.R.J. Artus, S. Seeger, A comprehensive study of concepts and phenomena of the nonspecific adsorption of  $\beta$ -lactoglobulin, *ChemPhysChem* 8 (2007) 862–872, <https://doi.org/10.1002/cphc.200600710>.
- K. Kubiak-Ossowska, M. Cwieka, A. Kaczynska, B. Jachimska, P.A. Mulheran, Lysozyme adsorption at a silica surface using simulation and experiment: effects of pH on protein layer structure, *Phys. Chem. Chem. Phys.* 17 (2015) 24070–24077, <https://doi.org/10.1039/C5CP03910J>.
- R.J.B.M. Delahaije, H. Gruppen, M.L.F. Giuseppin, P.A. Wierenga, Quantitative description of the parameters affecting the adsorption behaviour of globular proteins, *Colloids Surfaces B Biointerfaces.* 123 (2014) 199–206, <https://doi.org/10.1016/j.colsurfb.2014.09.015>.
- L. Pérez-Fuentes, C. Drummond, J. Faraudo, D. Bastos-González, Adsorption of milk proteins ( $\beta$ -casein and  $\beta$ -lactoglobulin) and BSA onto hydrophobic surfaces, *Materials (Basel)*, 10 (2017) 893, <https://doi.org/10.3390/ma10080893>.
- K. Kurpiewska, A. Biela, J.I. Loch, S. Świątek, B. Jachimska, K. Lewiński, Investigation of high pressure effect on the structure and adsorption of  $\beta$ -lactoglobulin, *Colloids Surfaces B Biointerfaces* 161 (2018) 387–393, <https://doi.org/10.1016/j.colsurfb.2017.10.069>.
- B. Jachimska, S. Świątek, J.I. Loch, K. Lewiński, T. Luxbacher, Adsorption effectiveness of  $\beta$ -lactoglobulin onto gold surface determined by quartz crystal microbalance, *Bioelectrochemistry* 121 (2018) 95–104, <https://doi.org/10.1016/j.bioelectrochem.2018.01.010>.
- R.A. Franco De Lima, M.B. de Jesus, C.M. Saia Cereda, G.R. Tofoli, L.F. Cabeça, I. Mazzaro, L.F. Fraceto, E. de Paula, Improvement of tetracaine antinociceptive effect by inclusion in cyclodextrins, *J. Drug Target.* 20 (2012) 85–96, <https://doi.org/10.3109/1061186X.2011.622400>.
- Y.H. Lee, N.S. Park, J.D. Kwon, J.S. Park, G.B. Shin, C.S. Lee, T.S. Jung, N.J. Choi, J.H. Yoon, J.S. Ok, U.C. Yoon, M.K. Bae, H.O. Jang, I. Yun, Amphiphilic effects of local anesthetics on rotational mobility in neuronal and model membranes, *Chem. Phys. Lipids* 146 (2007) 33–42, <https://doi.org/10.1016/j.chemphyslip.2006.12.002>.
- J.I. Loch, P. Bonarek, A. Polit, M. Jabłoński, M. Czub, X. Ye, K. Lewiński,  $\beta$ -Lactoglobulin interactions with local anaesthetic drugs – crystallographic and calorimetric studies, *Int. J. Biol. Macromol.* 80 (2015) 87–94, <https://doi.org/10.1016/j.ijbiomac.2015.06.013>.
- D. Agudelo, M. Beaugard, G. Bérubé, H.-A. Tajmir-Riahi, Antibiotic doxorubicin and its derivative bind milk  $\beta$ -lactoglobulin, *J. Photochem. Photobiol. B Biol.* 117 (2012) 185–192, <https://doi.org/10.1016/j.jphotobiol.2012.09.014>.
- S. Rudra, A. Jana, N. Sepay, B.K. Patel, A. Mahapatra, Characterization of the binding of strychnine with bovine  $\beta$ -lactoglobulin and human lysozyme using spectroscopic, kinetic and molecular docking analysis, *New J. Chem.* 42 (2018) 8615–8628, <https://doi.org/10.1039/C8NJ00810H>.
- J. Zhong, S. Fu, H. Yu, L. Zhou, W. Liu, C. Liu, S. Prakash, Antigenicity of  $\beta$ -lactoglobulin reduced by combining with oleic acid during dynamic high-pressure microfluidization: Multi-spectroscopy and molecule dynamics simulation analysis, *J. Dairy Sci.* (2018), <https://doi.org/10.3168/JDS.2018-14898>.
- A.H. Sneharani, J.V. Karakkat, S.A. Singh, A.G.A. Rao, Interaction of curcumin with  $\beta$ -lactoglobulin; stability, spectroscopic analysis, and molecular modeling of the complex, *J. Agric. Food Chem.* 58 (2010) 11130–11139, <https://doi.org/10.1021/jf102826q>.



- [29] J. Pronchik, J.T. Giurleo, D.S. Talaga, Separation and analysis of dynamic Stokes shift with multiple fluorescence environments: Coumarin 153 in bovine  $\beta$ -lactoglobulin a, *J. Phys. Chem. B* 112 (2008) 11422–11434, <https://doi.org/10.1021/jp802666n>.
- [30] M.H. Mehraban, S. Odooli, R. Yousefi, R. Roghanian, M. Motovali-Bashi, A.A. Moosavi-Movahedi, Y. Ghasemi, The interaction of beta-lactoglobulin with ciprofloxacin and kanamycin: a spectroscopic and molecular modeling approach, *J. Biomol. Struct. Dyn.* 35 (2017) 1968–1978, <https://doi.org/10.1080/07391102.2016.1203819>.
- [31] L. Sawyer, S. Brownlow, I. Polikarpov, S.Y. Wu,  $\beta$ -lactoglobulin structural studies, biological clues, *Int. Dairy J.* 8 (1998) 65–72, [https://doi.org/10.1016/S0958-6946\(98\)00021-1](https://doi.org/10.1016/S0958-6946(98)00021-1).
- [32] S. Shahraki, F. Shiri, Binding interaction of isoxsuprine hydrochloride and levothyroxine to milk  $\beta$ -lactoglobulin; from the perspective of comparison, *Int. J. Biol. Macromol.* 109 (2018) 576–588, <https://doi.org/10.1016/j.IJBIOMAC.2017.12.117>.
- [33] A. Albaugh, H.A. Boateng, R.T. Bradshaw, O.N. Demerdash, J. Dziedzic, Y. Mao, D.T. Margul, J. Swails, Q. Zeng, D.A. Case, P. Eastman, L.P. Wang, J.W. Essex, M. Head-Gordon, V.S. Pande, J.W. Ponder, Y. Shao, C.K. Skylaris, I.T. Todorov, M.E. Tuckerman, T. Head-Gordon, Advanced potential energy surfaces for molecular simulation, *J. Phys. Chem. B* 120 (2016) 9811–9832, <https://doi.org/10.1021/acs.jpcc.6b06414>.
- [34] K. Palczynski, A. Wilke, M. Paeschke, J. Dzubielka, Molecular modeling of polycarbonate materials: glass transition and mechanical properties, *Phys. Rev. Mater.* 1 (2017) 043804, <https://doi.org/10.1103/PhysRevMaterials.1.043804>.
- [35] I. Khalaila, C.S. Allardyce, C.S. Verma, P.J. Dyson, A mass spectrometric and molecular modelling study of cisplatin binding to transferrin, *Chembiochem* 6 (2005) 1788–1795, <https://doi.org/10.1002/cbic.200500067>.
- [36] J. Siepmann, N.A. Peppas, Modeling of drug release from delivery systems based on hydroxypropyl methylcellulose (HPMC), *Adv. Drug Deliv. Rev.* 64 (2012) 163–174, <https://doi.org/10.1016/j.addr.2012.09.028>.
- [37] H. Alonso, A.A. Bliznyuk, J.E. Gready, Combining docking and molecular dynamic simulations in drug design, *Med. Res. Rev.* 26 (2006) 531–568, <https://doi.org/10.1002/med.20067>.
- [38] Q. Feng, S. Wen, J. Deng, W. Zhao, DFT study on the interaction between hydrogen sulfide ions and cerussite (110) surface, *Appl. Surf. Sci.* 396 (2017) 920–925, <https://doi.org/10.1016/j.apsusc.2016.11.061>.
- [39] Q. Feng, S. Wen, J. Deng, W. Zhao, Combined DFT and XPS investigation of enhanced adsorption of sulfide species onto cerussite by surface modification with chloride, *Appl. Surf. Sci.* 425 (2017) 8–15, <https://doi.org/10.1016/j.apsusc.2017.07.017>.
- [40] S. Shahraki, A. Heydari, Binding forces between a novel Schiff base palladium(II) complex and two carrier proteins: human serum albumin and  $\beta$ -lactoglobulin, *J. Biomol. Struct. Dyn.* 36 (2018) 2807–2821, <https://doi.org/10.1080/07391102.2017.1367723>.
- [41] S. Shahraki, A. Heydari, M. Saeidifar, M. Gomroki, Biophysical and computational comparison on the binding affinity of three important nutrients to  $\beta$ -lactoglobulin: folic acid, ascorbic acid and vitamin K3, *J. Biomol. Struct. Dyn.* (2017) 1–15, <https://doi.org/10.1080/07391102.2017.1394222>.
- [42] I. Brandariz, E. Iglesias, Potentiometric characterisation of cyclodextrin inclusion complexes of local anaesthetics, *Supramol. Chem.* 23 (2011) 607–614, <https://doi.org/10.1080/10610278.2011.593632>.
- [43] M.A. Nouairi, T. Fergoug, M. Azayez, H. Boujoudes, C. Zemat, Y. Bouhadda, Experimental and theoretical study of tetracaine-hydrochloride  $\beta$ -cyclodextrin complexation, *J. Mater. Environ. Sci.* 8 (2017) 1589–1598.
- [44] M. Bello, G. Gutiérrez, E. García-Hernández, Structure and dynamics of  $\beta$ -lactoglobulin in complex with dodecyl sulfate and laurate: a molecular dynamics study, *Biophys. Chem.* 165–166 (2012) 79–86, <https://doi.org/10.1016/j.bpc.2012.03.009>.
- [45] B. Ghalandari, A. Divsalar, A.A. Saboury, T. Haertlé, K. Parivar, R. Bazl, M. Eslami-Moghadam, M. Amanlou, Spectroscopic and theoretical investigation of oxali-palladium interactions with  $\beta$ -lactoglobulin, *Spectrochim. Acta Part A Mol. Biomol. Spectrosc.* 118 (2014) 1038–1046, <https://doi.org/10.1016/j.SAA.2013.09.126>.
- [46] D. Agudelo, M. Beauregard, G. Bérubé, H.-A. Tajmir-Riahi, Antibiotic doxorubicin and its derivative bind milk  $\beta$ -lactoglobulin, *J. Photochem. Photobiol. B Biol.* 117 (2012) 185–192, <https://doi.org/10.1016/j.jphotobiol.2012.09.014>.
- [47] J.I. Loch, P. Bonarek, A. Polit, S. Świątek, M. Dziedzicka-Wasylewska, K. Lewiński, The differences in binding 12-carbon aliphatic ligands by bovine  $\beta$ -lactoglobulin isoform a and B studied by isothermal titration calorimetry and X-ray crystallography, *J. Mol. Recognit.* 26 (2013) 357–367, <https://doi.org/10.1002/jmr.2280>.
- [48] F. Zsila, E. Hazai, L. Sawyer, Binding of the pepper alkaloid piperine to bovine  $\beta$ -lactoglobulin: Circular dichroism spectroscopy and molecular modeling study, *J. Agric. Food Chem.* 53 (2005) 10179–10185, <https://doi.org/10.1021/jf051944g>.
- [49] Q. Feng, S. Wen, W. Zhao, Y. Wang, C. Cui, Contribution of chloride ions to the sulfidization flotation of cerussite, *Miner. Eng.* 83 (2015) 128–135, <https://doi.org/10.1016/j.MINENG.2015.08.020>.
- [50] Q. Feng, W. Zhao, S. Wen, Surface modification of malachite with ethanediamine and its effect on sulfidization flotation, *Appl. Surf. Sci.* 436 (2018) 823–831, <https://doi.org/10.1016/j.apsusc.2017.12.113>.
- [51] Q. Feng, W. Zhao, S. Wen, Q. Cao, Activation mechanism of lead ions in cassiterite flotation with salicylhydroxamic acid as collector, *Sep. Purif. Technol.* 178 (2017) 193–199, <https://doi.org/10.1016/j.seppur.2017.01.053>.